Monatshefte für Chemie - Chemical Monthly (2024) 155:361–367
https://doi.org/10.1007/s00706-024-03185-5

ORIGINAL PAPER

Hybrid organic–inorganic fibers for solid-state batteries

Václav Procházka[1] · Martin Havlík Míka[1] · Jan Kočí[1] · Nikola Klusoňová[1] · Eliška Sedláčková[1]

Received: 27 September 2023 / Accepted: 12 February 2024 / Published online: 6 March 2024

Abstract
This study is dedicated to the acquisition and quantification of processing parameters essential for the fabrication of customizable organic–inorganic hybrid nano/microfibers through electrospinning. These fibers are generated from suspensions comprising active electrode materials utilized in the construction of all solid-state batteries. Owing to the catalytic properties exhibited by certain electroactive materials and the coagulation tendencies stemming from the presence of various particles, there exists a limited operational interval within which stable fibers can be produced while maintaining the suspension at a suitable viscosity. Our second goal was to ascertain the relationship between the quality of the resulting fibers and the spinnability of the suspension, particularly regarding its electrical conductivity. Solutions and suspensions were studied with help of ^{29}Si NMR spectroscopy, EIS, and conductometry, fiber morphology with confocal and electron microscopy.

Graphical abstract

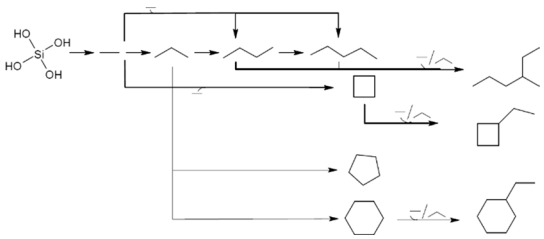

Keywords Electrospinning · Inorganic polymers · Material science · Nanostructures · NMR spectroscopy

Introduction

Sol–gel represents a convenient approach for producing highly homogeneous glass and ceramics, typically at temperatures significantly lower than their respective melting or fusion points [1]. According to research findings, the structure of the resultant products is liable upon the initial stages of the sol–gel transformation, namely hydrolysis and polymerization. Hydrolysis (Eq. 1) occurs when the silica precursor, primarily tetraethyl orthosilicate (TEOS), is combined with water in a common solvent, typically ethanol. In theory, complete hydrolysis would yield silicic acid (H_4SiO_4); however, in practice, this ideal state is not realized. Instead, a range of intermediates is generated, rendering the kinetic description of the process exceedingly complex:

$$Si(OC_2H_5)_4 + H_2O \rightarrow Si(OH)_n(C_2H_5)_{4-n} \quad (1)$$

Polymerization (Eq. 2) reaction generates water, complicating reaction description even more; therefore, hydrolysis reaction can be described only qualitatively. Water generation keeps hydrolysis reaction running but the reaction mechanics is determined by used catalyst. Acid catalysis results in more problematic subsequent hydrolysis leading to more linear structures. Base catalysis promotes subsequent hydrolysis, leading to branched clusters. Water content is also controlling element of reaction. Low water acid catalyzed content solutions produce linear polymer chains, and higher water content sols lead to more branched structures [2–4]:

✉ Václav Procházka
Vaclav.Prochazka@vscht.cz

[1] Institute of Glass and Ceramics, University of Chemistry and Technology, Prague, Czech Republic

$$2Si(OH)_n(C_2H_5)_{4-n} \rightarrow R_n - Si - O - Si - R_n + C_2H_5OH \quad (2)$$

Studies have shown that clusters formed even in acid catalyzed sol–gel reactions are usually relatively short 5–7 Si atoms long, slightly branched chains or cyclic structures mostly 5–6 Si atom units [5] as shown in Fig. 1. Branched chains are responsible for earlier irreversible gelation of sol by restricting flow than in case of linear chains.

For spinning purposes, sol is usually mixed with high molecular weight polymers acting as carrier or matrix increasing spinnability, fiber uniformity and decreasing fiber diameter. Spinnability is generally referred to ability to form uniform (no beads) and uniformly distributed fibers. The literature report much better results for silica precursors mixed with polymers [7, 8]; however, there are studies forming high-quality nanofibers using pure sols [9].

Electrospinning process is also well known and is quite wide-spread method of production of nanomaterials such as nanofibers (NF) or nanorods (NR). Since its first development in 1882, there are numerous advances, most in last decades. It has become a versatile method for creating 1D, 2D, and 3D structures with application in electrotechnical, medical, or bioengineering industries [10–12]. In recent years, it has been used more frequently to produce functional nanofibrous materials from metal oxides combining sol–gel method and electrospinning.

Main advantage of this process lies in relative ease to modify properties of produced fibers, low cost, versatility, and easy fiber alignment. Moreover, based on fiber processing, it is easy to produce inorganic fibers either amorphous or crystalline.

Basic principle of electrospinning lies in electrostatic repulsion of charge spun polymer particles causing capillary jet or droplet elongation. The balance between electrostatic repulsion and surface tension leads to formation of so-called Taylor cone. When electrostatic force overcomes surface tension, narrow jet is ejected from the droplet. After ejection, electrostatic repulsion becomes stronger thanks to evaporation of solvent [13].

The electrospinning mechanisms are complex processes. First theoretical model was created by Taylor, and later many more were developed and derived, mostly to include development of needleless processes [14–21]. Those are based on four steady-state equations governing basics of the whole process [13]. With the right processing parameters, it is possible to obtain fibers with diameters from less than 1 nm to tens of micrometers depending on particle size [22]. Some spinning solutions suitable for mass production can generate fibers 36 nm, and lower diameters are reported to be only achieved in laboratory conditions. There are numerous properties determining fiber properties and structure, generally, spinning parameters are divided into 3 categories: (1) ambient conditions (e.g., temperature, humidity, pressure, air convection): these can be easily controlled and are independent on other categories; (2) solution properties (e.g., viscosity, conductivity, surface tension, solvent), and (3) process parameters (spinneret geometry, collector geometry, applied voltage, flow rate, collector distance). Thomson et al. have created model for prediction and process control and designated 13 major parameters [21, 22]. Most process parameters effect primarily 1D structure morphology, but with change of collector geometry, it is possible to modify 3D arrangement. Generally, products are nonwoven mats but with use of rotating collectors aligned fibers are easily obtainable. When there is need for woven-like structure, it is possible to use paired electrodes with controlled charge. Main disadvantage of the basic process is low productivity. The simplest way to

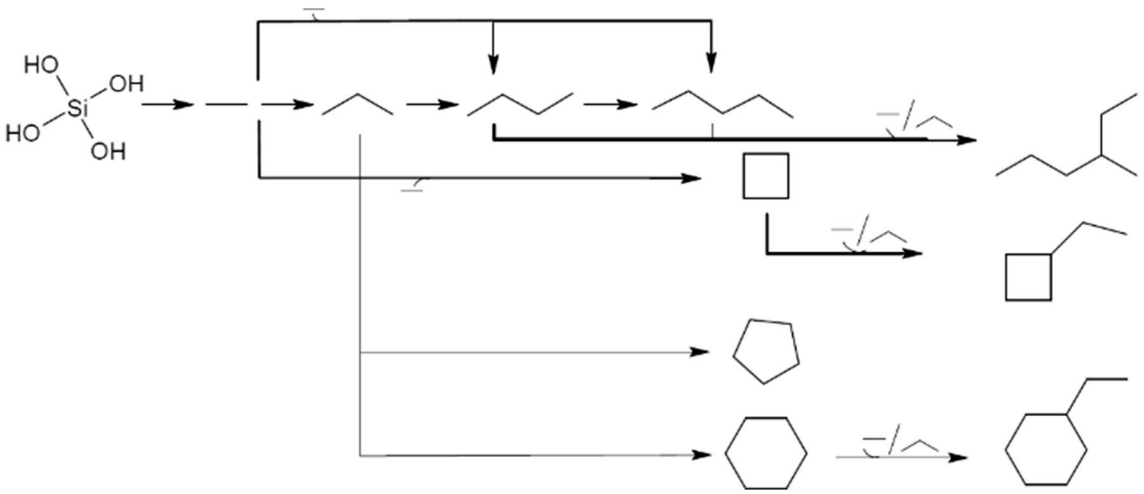

Fig. 1 Theoretical schematics of hydrolyzed species condensation [6]

increase it would be adding additional spinnerets; however, quality of the final structure may suffer. Therefore, several "needleless" designs were created [23, 24].

Some of aforementioned properties have known effect on fiber properties; others such as conductivity are disputed over its effect. Some studies show positive effect of high conductivity on fiber formation (smaller diameter and uniformity) [13], some report to have negative [25] and some even report conductivity having no effect at all or a necessity for use of semiconductive solution.

There are few studies reporting use of electrospun silica fibers as carriers for active electrode materials as well as matrix for battery components. Metal oxides are known for their high capacitance; however, low conductivity is considered as too great obstacle for general use. The usual concept is to dope carbon-based material such as carbon NF or NT or conductive polymer with material with higher energy density, mostly silicon. More research is based on carbonization of fibrous polymer mats filled with active material [7, 26–28].

Results and discussion

^{29}Si NMR

Although numerous investigations have been undertaken, they are often designed to examine the kinetics of stoichiometric systems or systems with an excess of water, with the intent of minimizing complexity. In this study, NMR spectroscopy primarily serves as a tool to establish correlations between empirical and conductometry data, while also facilitating the prediction and control of process parameters, thereby expediting the manufacture of fibers. The detailed characterization of the generated species was deemed unnecessary, given that the sol served solely as a precursor for the solid product and was subsequently subjected to calcination. Notably, Depla's research [5] has indicated that Q^4 motifs are not substantially represented in the system. For the sake of simplicity in evaluating the measurements, only general Q motifs (both cyclic and linear) were taken into account. Peaks were identified based on known ^{29}Si chemical shifts listed in Table 1.

The measurements conducted (see Fig. 2) reveal that following an initial rapid evolution of products, the ratio of Q^2 to Q^3 motifs appears relatively stable, with chains being the primary variable increasing in length (as depicted in Fig. 3).

During longer term measurements, it becomes evident that the relative concentration of Q^3 structures exhibits gradual growth. Solutions featuring Q^3 concentrations exceeding 30% experience gelation within minutes of introducing electroactive particles, rendering the material unsuitable for its intended purpose.

Table 1 The relationship between ^{29}Si chemical shifts ($-\delta$ ppm) relative to TMS and silicate structures

	$-\delta$/ppm	Silicate structure
M^{OH}	12.3–14.0	HO–Si*$(CH_3)_2$–O–[Si$(CH_3)_2$–O–]$_n$–Si(CH_3)–OH
D(Q)	16.3–17.7	$(–O–)_3$Si–O–Si*$(CH_3)_2$–O–Si≡
D_{4C}	18.9–19.4	[Si*$(CH_3)_2$–O–]$_4$ (cyclic)
D	20.1–22.0	HO–Si(CH_3)–O–[Si*(CH_3)–O–]$_n$–Si$(CH_3)_2$–OH
Q^0	79.0–82.0	Si*$(OR)_4$
Q^1	85.0–89.0	Si*$(OR)_3$(–O–Si≡)
Q^2	91.0–97.0	Si*$(OR)_2$(–O–Si≡)$_2$
Q^3	100.0–103.0	Si*(OR)(–O–Si≡)$_3$
Q^4	108.0–110.0	Si*(–O–Si≡)$_4$
	R = H or C_2H_5	

Fiber morphology

The investigation into fiber morphology encompassed pristine fibers and those containing filler at concentrations of 8.3%, 25%, and 50% w/w (filler/TEOS). It was observed that when spinning solutions with short aging times were employed, the fibers displayed a tendency to coalesce, forming thick membranes instead of the desired nonwoven nanofibrous mat, regardless of whether they contained filler or not. This phenomenon persisted even when PVP was included in the solution. Subsequent calcination of these membranes resulted in the loss of flexibility, likely attributable to the substantial internal stresses induced by rapid sample shrinkage, ultimately leading to fracture (Fig. 4).

Based on these observations, we determined that a minimum solution aging period of 100 h at 5 °C was necessary to achieve the formation of stable fibers. Uniform fibers were consistently obtained with solutions aged for nearly 30 days. Beyond this duration, fibers remained uniform with minimal bead formation, and filler particles were uniformly dispersed throughout.

The presence of filler material exerted a significant influence on spinning stability. Specifically, solutions containing 8.3% and 25% filler maintained a stable Taylor cone during the electrospinning process. However, when the filler content was increased to 50%, the spinning process became unstable. Instead of yielding continuous fibers, the spinneret exhibited pulsating behavior, ejecting fibrous agglomerates (Fig. 5).

Sol conductivity and EIS

Conductivity of spinning polymer solution is deemed as one of the main controlling parameters of electrospinning process. Its values are constantly changing with aging of the

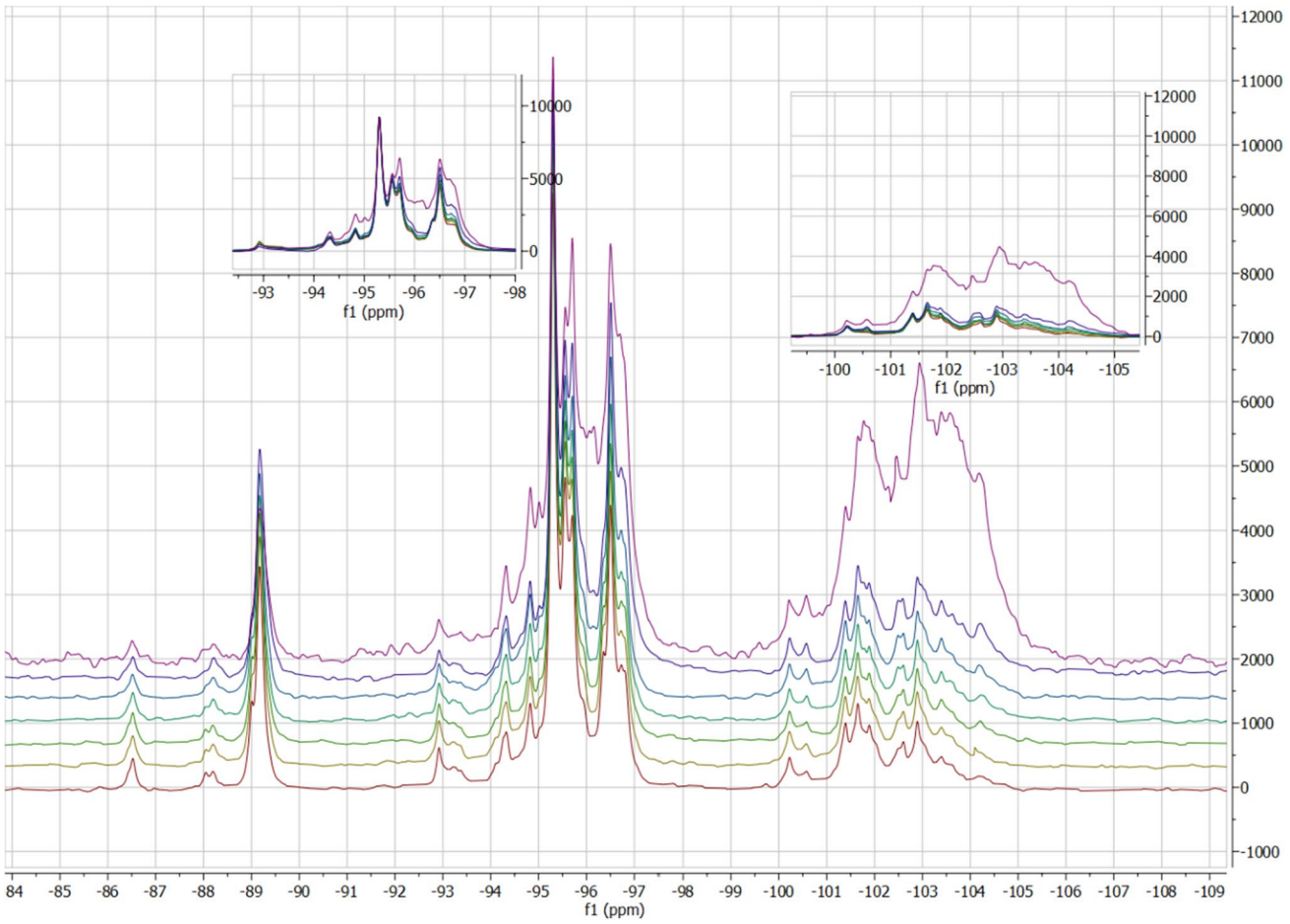

Fig. 2 ^{29}Si NMR spectra of TEOS sol aging

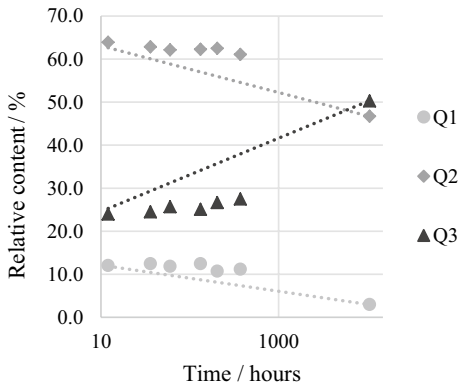

Fig. 3 Q motifs relative content development

sols and filler addition was expected to change conductivity significantly.

During initial stages, aging of precursor sol has stable conductivity with median value of 30.53 μS cm^{-1}. TEOS-PVP mixture has conductivity of 11.13 μS cm^{-1}. During later stages of aging, approximately after 250 days, sol conductivity starts to decrease significantly. However, the addition of PVP solutions is still spinnable. In these later stages, short workability times, minutes to approximately 20 min after particles addition, are the main issue (Fig. 6).

The addition of silicon particles decreased conductivity (Fig. 7); however, changes in fiber formation are minor and effect can be omitted opposed to viscosity changes reported by Kočí on ABAF conference. Furthermore, the differences in conductivity for different particles concentrations were within observational error.

Even though conductivity changes caused by particles addition can be neglected as electrospinning processing parameter, it is useful as controlling mechanism of workability for TEOS solution, much better than use of NMR spectroscopy.

As for EIS, suspension with 8.3% was used for creating equivalent circuit model (ECM) as shown in Fig. 8. This particular model exhibited satisfactory agreement with experimental data (Fig. 9). Nevertheless, minor modifications may be necessary in subsequent investigations. Parameters of the ECM were calculated and are listed in Table 2.

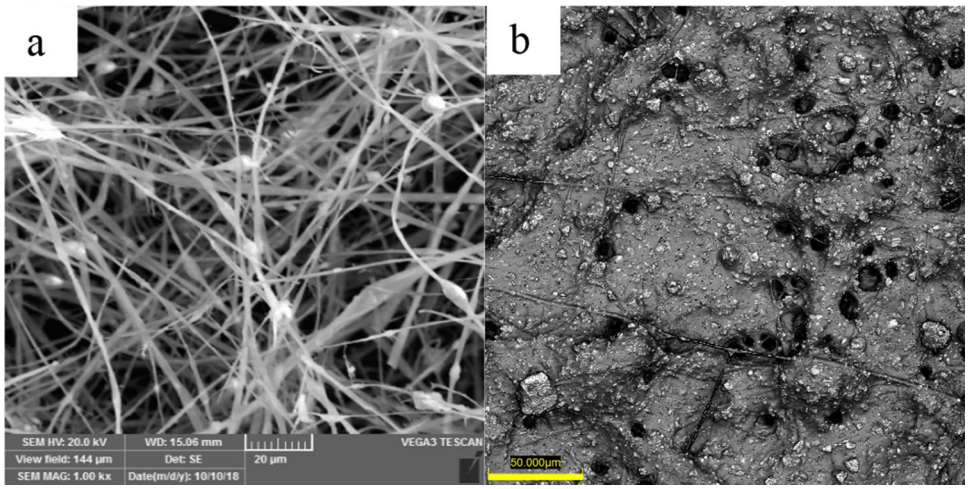

Fig. 4 **a** Fibers formed from 14 to 30 days aged sols, no filler; **b** layer formed from 8 days aged sols with filler

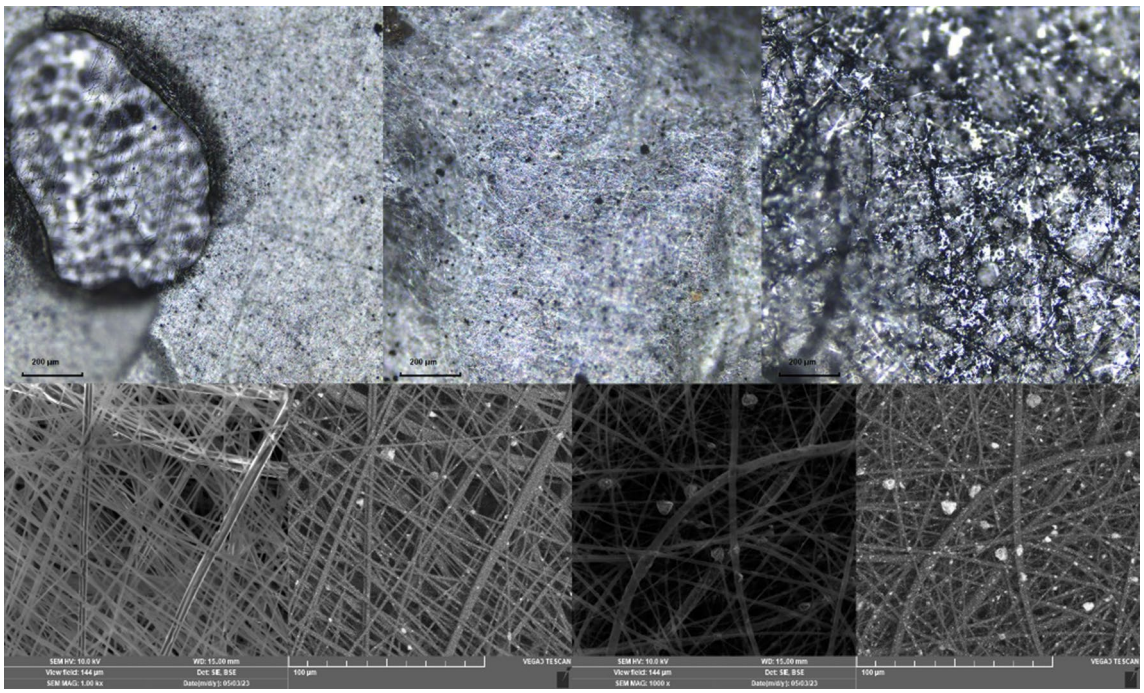

Fig. 5 **a** Fibers with 8.3% filler content; **b** fibers with 25% filler content; **c** fibers with 50% filler content; **d** fibers without filler content; **e** SEM image of fibers with 8.3% filler content; **f** SEM image of fibers with 25% filler content; **g** SEM image of fibers with 50% filler content

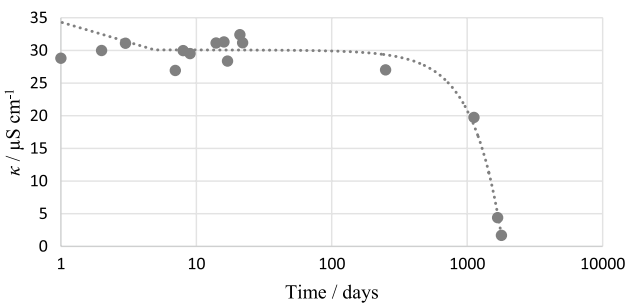

Fig. 6 Sol conductivity in time

Conclusion

The addition of active particles exerts an influence on the morphology of electrospun fibers. However, it is noteworthy that the disparities in electrical conductivity resulting from these additions are relatively minor. As such, the impact of altered conductivity can be considered negligible for our specific material. The reduction of the spinnability of the suspension is more likely attributable to modifications in fluid dynamics, particularly the notable increase in viscosity.

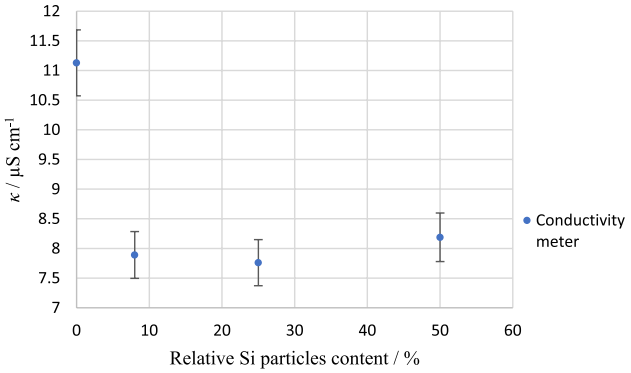

Fig. 7 Sol conductivity dependence on Si content

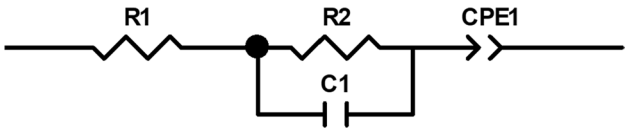

Fig. 8 Used equivalent circuit

Our investigations, including morphology analysis, ^{29}Si NMR spectroscopy, EIS, and conductivity data, align with empirical observations. These collective findings converge to indicate that the optimal working interval, where the suspension demonstrates its highest spinnability, falls within a sol aging period of 1–5 months at 5 °C. During this timeframe, the presence of beads in the resulting fibers is either nearly absent or attributed to the encapsulation of particles. Created ECM will be used to evaluate more samples and create even more precise working conditions in future projects.

Table 2 Established ECM parameters according to NLSM fit

	Value	Error	Relative error
R_1/mΩ	68.10	373.21	54.88
R_2/mΩ	7588.00	361.98	4.77
C_1/F	1.47×10^{-10}	1.49×10^{-11}	10.14
A/F	4.52×10^{-6}	5.72×10^{-8}	1.27
α	0.74	3.70×10^{-3}	0.49

Experimental

Tetraethyl orthosilicate (TEOS), poly (vinyl pyrrolidone) (PVP) (M_w 1,300,000), hydrochloric acid, and ethanol were used. Deionized water was used throughout the experiment. NMC spinels were acquired from discarded batteries and silicon from discarded solar panels.

Experiment

The suspensions for electrospinning were prepared by controlled condensation of TEOS at low temperatures. TEOS was dissolved in ethanol and then HCl, water, and ethanol were added dropwise and continuously stirred. During the mixing, solution was kept at temperatures between 20 and 30 °C to prevent particles precipitation, which occasionally occurred at temperatures over 35 °C. Sols were then kept in fridge to age. Prior to electrospinning PVP

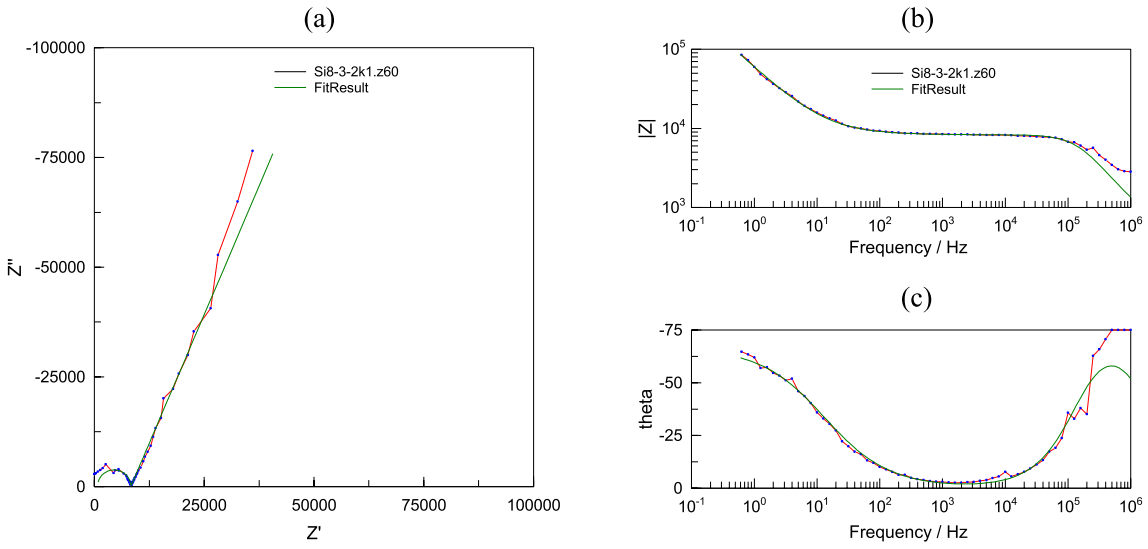

Fig. 9 Impedance measurement. **a** Nyquist impedance plot; Bode plots of **b** absolute value of impedance; **c** phase angle θ as function of frequency

dissolved in ethanol 1:6 W/W to modify viscosity and increase spinnability and active particles were added to the mixture. Substoichiometric composition (TEOS:water) was chosen due to its inherent longer gelation times caused by promoted linear chains formation. These solutions are more resistant to premature gelation after electroactive particles addition.

Electrospinning was conducted on SKE EF050, with nozzle diameter 0.8 mm, applied voltage 25 kV, flow rate 1 cm^3/h, collector (aluminum) distance 12 cm and covered with glassfibre mesh. Prepared fibrous mats were calcinated in muffle furnace at temperatures 650 °C and 1000 °C in air atmosphere.

Condensation reactions during aging within sols were analyzed with ^{29}Si NMR spectroscopy. Spectra were recorded with Bruker Avance III (11.75 T). Conductivity of sols was determined using two-probe impedance method with stainless steel electrode 0.81 mm thick.

Particles were prepared on E-Max high-energy ball mill by dry milling in zirconia jar and balls with 1:30 sample: milling balls ratio, 800 rpm for 10 min. Milled particles were sieved on 40 µm sieve and for measurement dispersed and ultrasonicated in isopropanol.

Morphology of resulting fibers and particle size distribution were analyzed using confocal laser microscope LEXT OLS5000 SAF and SEM TESCAN VEGA 3 LMU.

Electrochemical impedance spectroscopy was measured on Metrohm Autolab, and conductivity measurements were conducted on Motech MT4090 meter.

Funding Open access publishing supported by the National Technical Library in Prague.

Data availability The participants of this study did not give written consent for their data to be shared publicly, so research supporting data is not available.

References

1. Schmidt H (1988) J Non Cryst Solids 100:51
2. Assink RA, Kay BD (1988) J Non Cryst Solids 107:35
3. Ro JC, Chung IJ (1989) J Non Cryst Solids 110:26
4. Klein LC (1985) Annu Rev Mater Sci 15:227
5. Depla A, Lesthaeghe D, van Erp TS, Aerts A, Houthoofd K, Fan F, Li C, Van Speybroeck V, Waroquier M, Kirschhock CEA, Martens JA (2011) J Phys Chem C 115:3562
6. Procházka V, Míka MH, Kočí J (2022) J Phys: Conf Ser 2382:012018
7. Sheng J, Ma C, Ma Y, Zhang H, Wang R, Xie Z, Shi J (2016) Int J Hydrogen Energy 41:9383
8. Liu Y, Sagi S, Chandrasekar R, Zhang L, Hedin NE, Fong H (2008) J Nanosci Nanotechnol 8:1528
9. Choi S-S, Lee SG, Im SS, Kim SH, Joo YL (2003) J Mater Sci Lett 22:891
10. Zhou J, Nie Y, Jin C, Zhang JX (2022) ACS Biomater Sci Eng 8:2258
11. Chen Y, Shafiq M, Liu M, Morsi Y, Mo X (2020) Bioact Mater 5:963
12. Mi H-Y, Jing X, Huang H-X, Turng L-S (2017) Mater Lett 204:45
13. Angammana CJ, Jayaram SH (2011) IEEE Trans Nanotechnol 47:1109
14. Eddy RD, Taylor CG, Dye KE, Johnson SR, Miles BH (1966) Synthesis and characterization of model polymers for use in the investigation of char forming heat shields
15. Fisch W, Hofmann W (1961) Makromol Chem 44:8
16. Hohman MM, Shin M, Rutledge G, Brenner MP (2001) Phys Fluids 13:2221
17. Huang Z-M, Zhang YZ, Kotaki M, Ramakrishna S (2003) Compos Sci Technol 63:2223
18. Rafiei S, Maghsoodloo S, Noroozi B, Mottaghitalab V, Haghi AK (2013) Cell Chem Technol 47:323
19. Taylor CG, Pendleton EL (1969) J Macromol Sci Part A Pure Appl Chem 3:453
20. Yarin AL, Koombhongse S, Reneker DH (2001) Jpn J Appl Phys 89:3018
21. Thompson CJ, Chase GG, Yarin AL, Reneker DH (2007) Polymer 48:6913
22. Saleh Hudin HS, Mohamad EN, Mahadi WNL, Muhammad Afifi A (2018) Mater Manuf Process 33:479
23. Li D, Xia Y (2004) Adv Mater 16:1151
24. Kameoka J, Orth R, Yang Y, Czaplewski D, Mathers R, Coates GW, Craighead HG (2003) Nanotechnology 14:1124
25. Chen L-J, Liao J-D, Lin S-J, Chuang Y-J, Fu Y-S (2009) Polymer 50:3516
26. Zhang B, Kang F, Tarascon J-M, Kim J-K (2016) Prog Mater Sci 76:319
27. Kim B-H, Yang KS, Woo H-G (2011) Electrochem Commun 13:1042
28. Favors Z, Bay HH, Mutlu Z, Ahmed K, Ionescu R, Ye R, Ozkan M, Ozkan CS (2015) Sci Rep 5:8246